THE IMPACT OF PULSE PLASMA TREATMENT ON THE MICROHARDNESS OF STEEL 40X10C2M: EXPERIMENT AND NUMERICAL SIMULATIONS†

Nikolay A. Savinkov[a,*], Oleh M. Bulanchuk[b], Aleksander A. Bizyukov[c]

aAzovskyi Maritime Institute of NU «OMA», 19 Chornomors'ka str., Mariupol, 87517, Ukraine
bDonetsk State University of Management , 58 Karpinskogo str., Mariupol, 87513, Ukraine
cV.N.Karazin Kharkiv National University, 4 Svobody Sq., Kharkiv, 61022, Ukraine.
*Corresponding Author: nik.sv2010@yandex.ua, phone: +380-98-376-03-75
Received June 6, 2021; revised July 29, 2021; accepted August 28, 2021

This paper presents a study of operating characteristics of steel 40X10C2M after treatment it of high-energy plasma pulses. The steel is used to manufacture the elements of ships' power plants. For pulsed plasma treatment of steel samples, we used an electrothermal plasma accelerator (ETPA). A high-current pulsed high-pressure arc discharge was initiated in a restricted dielectric chamber of ETPA. The discharge duration was 1.4 ms, the maximum current reached the value of 5 kA, the discharge voltage was up to 5 kV. We investigated the microhardness and microstructure of the processed (modified) layer and determined the optimal parameters of steel processing that provide the best characteristics of the modified layer when the microhardness increases by $\approx$ 5 times. Microhardness maxima were discovered in the depth of the modified layer. The paper studies the possibilities of controlling the maxima localization to form the desired performance characteristics of the treated layer. Mathematical modeling of rapid pulsed heating of the steel surface layer is performed within the framework of the two-phase "melt-solid" model, taking into account the dynamics of the thermodynamic characteristics of steel. For this purpose, we used the classical equation of thermal conductivity with varying steel parameters: density, heat capacity, and coefficient of thermal conductivity during the transition of a substance from the liquid to the solid phase. Within the chosen mathematical model, numerical calculations of the rapidly pulsed heating phenomenon of the steel surface were performed, taking into account melting and solidification in the Comsol Multiphysics package using the finite element method. The numerical simulation results are in good agreement with the experimental distribution of the microhardness of the treated steel layer deep into the sample.
Keywords: plasma treatment, modified layer, microhardness, microstructure, thermal conductivity equation, melting and solidification, melt cooling rate.
PACS: 07.90.+c; 52.90.+z; 44.05.+e; 02.60.-x; 68.35.Rh; 61.50.Ks

The surface treatment of metals and alloys using high-energy electron and ion beams, laser radiation, high-temperature thermal plasma stream was widely used to modify the properties of a thin surface layer of various materials [1-3]. In this case, the modification of the surface layer occurs due to a whole complex of processes: rapid heating and cooling (quenching), formation of defects and structural stresses, ion implantation, deposition, epitaxy of atoms and molecules, and radiation-stimulated diffusion. Such processing can result in the surface layer melting of the metal followed by ultrafast crystallization and the formation of a modified layer with a thickness of (10-200) microns [4-6]. As a consequence of various structural and phase transformations occurring in the modified layer, many operational characteristics of the product are improved, such as microhardness, durability, heat, corrosion, and erosion strength.

Here it is necessary to highlight the pulse-plasma technology (PPT) [2,7] for material processing, the advantages of which are high heating and cooling rates of the metal surface (106-108 K/s), the ability of varying the plasma stream parameters (number of pulses, specific power) and the ability of creating layered structures with various phase composition. Another advantage is the ability to impact the item locally by pulsed plasma.

In various works researchers observed an increase in the microhardness of the modified layer and an ambiguous change of the microhardness along the depth of the layer. For instance, in work [7] the microhardness maxima on the surface of the modified metal layer and a decrease of microhardness deep into this layer up to values typical for the base were obtained. The electro-explosive boron-copper plating of the steel-45 surface resulted in a threefold increase of the surface microhardness [8]. Microhardness of 17-4PH stainless steel behaves oppositely and increases linearly along with the layer depth (up to 600 microns) after steel treatment by pulsed energy streams [9]. In work [10], when processing steel with high-current electron beams, the microhardness values decreased exponentially along with the depth of the modified layer. Thus, using PPT the authors observed contractionary behavior of microhardness with the depth of the treated layer, so that aspect demands additional investigations.

The use of PPT can be associated with both "heating-cooling" processes and phase transformations of the first kind: melting and solidification. The size of the molten zone, the processes of transferring the heat stream into the interior, and the cooling rate depend on the modes of plasma exposure and the thermophysical properties of the processed material [11]. To determine the influence of each of these factors, it is necessary to simulate the space-time distributions of the temperature and the dynamics of phase transitions with the subsequent comparison with experimental data. For this purpose various mathematical models [12-15] are used. Some of the models can be solved analytically [14], but most of them are solved numerically [6,12,13]. In this case it is possible to consider the single-phase model of

transmission of heat to solid during the "fast heating – cooling" process (that is, without melting the surface [14.15]) or a two-phase model of "rapid heating and melting of the surface layer–hardening" [16.17])

Numerical calculations of heat transfer processes in two-phase systems during the solidification process of the molten surface layer obtained by many authors [12,13,16,17] assumed that the thermodynamic characteristics of the medium remain stationary. In fact, in two-phase models, it is necessary to take into account the dynamics of the main thermodynamic characteristics of a substance (density, heat capacity, coefficient of thermal conductivity). The simulation also did not determine the cooling rate $\Delta T / \Delta t$ of the melt and its distribution over the depth of the molten zone. The cooling rates determine the strength properties of the treated layer, and the cooling rate should correlate with the microhardness values.

The purpose of this work is, first, to study the microhardness and microstructure of the modified layer of 40X10C2M steel after the pulsed plasma treatment; second, to obtain the distribution of microhardness over the depth of the treated layer; third, to simulate numerically the rapid pulse heating process of the steel layer surface in the framework of the two-phase model "melt - solid" while taking into account the dynamics of thermodynamic characteristics of steel; forth, to compare the simulation results with experimental data.
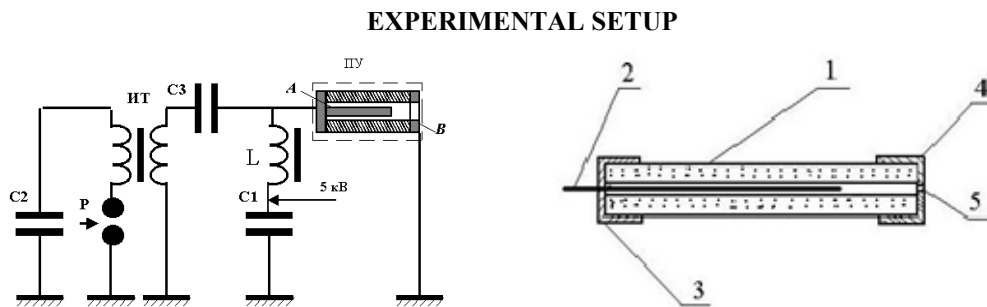
EXPERIMENTAL SETUP

Figure 1. The electrothermal plasma accelerator (right)

and its electrical power supply circuit (left)For pulsed plasma treatment of steel samples, we used an electrothermal plasma accelerator (ETPA) – Fig. 1. A high-current pulsed high-pressure arc discharge was initiated in a restricted dielectric chamber (1) at atmospheric pressure between a consumable rod-shaped iron cathode (2) and an axially located ring-shaped anode (4) [18]. The edges of dialectical chamber is molded by metallic barrels 3 and 4. The anode was grounded, and we applied the voltage from the capacitive energy storage to the rod cathode. The discharge duration was 1.4 ms, the maximum current reached 5 kA, the discharge voltage was up to 5 kV, and the maximum stored energy in a pulse was (20-37) kJ. The working substance entered the discharge chamber due to the intense evaporation of the iron cathode. As a result, the chamber pressure rises for a short time up to (100-150) atm. The discharge led to the appearance of liquid metal in the form of vapor and plasma of the cathode medium. In this case, a pulsed injection of a dense gas-plasma beam ocurred through the hole (5) in the ring-shaped anode in the direction of the sample under study. According to the obtained estimations, the plasma parameters: density and temperature approximately 10^{16} cm^{-3} and (1-2) eV, respectively.

EXPERIMENTAL RESULTS AND DISCUSSION

As specimens, we used plates with dimensions of (0.5x2x2) cm made of 40X10C2M steel. The samples were installed outside the discharge chamber near the anode and irradiated with one or more ETPA pulses. Before irradiation, the samples underwent standard thermal treatment: quenching and low tempering. We analyzed the modified layer microstructure of the processed specimens at a metallographic microscope "Neophot-21". The Vickers microhardness of the samples was measured using a PMT-3 device.

The microstructure investigations, thickness, and microhardness of the modified layer of irradiated samples were carried out depending on the parameters of pulsed plasma treatment. The optimal distance from the plasma source to the specimen surface was determined experimentally on the level of 30 mm, at optimal discharge voltage of the ETPA of 4 kV. For these distance and voltage value, the power density on the sample surface was calculated as $q_0 = W / S \approx 10^9$ W/m^2. Such a power density value provided the maximum rate of the "heating-ultrafast cooling" cycle of the near-surface layer. The quick cycle ensured a formation of dispersed alloyed crystal structure with a high dislocation density, and a hardened modified layer was formed. Fig. 2 shows the microstructure of the modified steel layer after pulsed plasma treatment. As we can see, the best structure is formed when the number of pulses is N = 4, the discharge voltage is U = 4.0 kV and the distance from the source to the sample is 30 mm (Fig. 2b).

As the distance from the ETPA to the sample surface decreases or as the discharge voltage increases to the maximum possible value of 5 kV, the power density increases, but the cathode starts ejecting metal droplets. Finally, the modified layer microstructure worsens and becomes loose and inhomogeneous (Fig. 2c). At a greater distance from the source to the sample, the thickness of the modified layer decreases (Table 1). At a distance of $l = 70$ mm, the thickness drops to ≈ 53 μm.
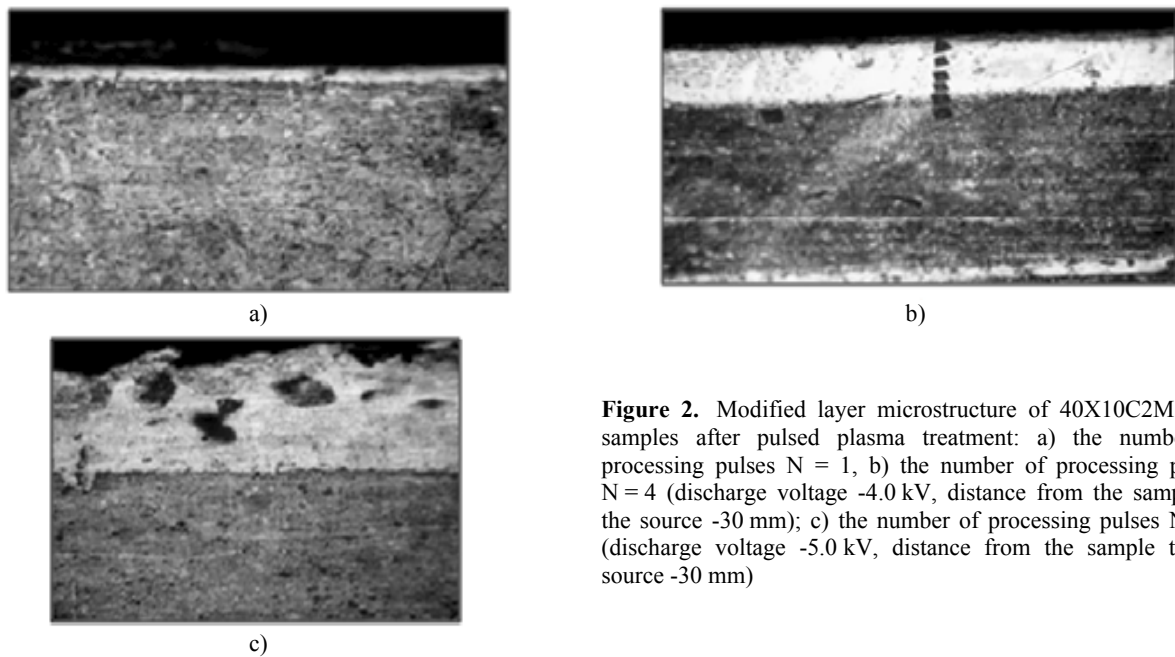
a)

b)

c)

Figure 2. Modified layer microstructure of 40X10C2M steel samples after pulsed plasma treatment: a) the number of processing pulses N = 1, b) the number of processing pulses N = 4 (discharge voltage -4.0 kV, distance from the sample to the source -30 mm); c) the number of processing pulses N = 6 (discharge voltage -5.0 kV, distance from the sample to the source -30 mm)

Table 1. Values of the modified layer average thickness of steel samples at various modes of pulsed plasma treatment.

The discharge voltage of the ETPA, kV	The number of processing pulses	The distance from the plasma source to the sample, mm	The modified layer average thickness, μm
2.0	1	30	18.4
2.5	1	30	25.6
3.0	1	30	27.1
4.0	1	30	35.5
4.0	3	30	75.8
4.0	4	30	118.8
4.0	5	30	128.1
4.0	6	30	125.5
4.0	7	30	128
4.0	8	30	122.7
4.0	4	70	53

Table 1 shows the results of pulsed plasma treatment of 40X10C2M steel samples. The table shows the modified layer's average thickness at different power densities load of the plasma stream to the sample surface. Influence of the power density was determined by three factors: 1) the discharge voltage of the ETPA; 2) the number of processing pulses; 3) the distance from the plasma source to the sample.

From the analysis of the data in the table, it is advisable to increase the number of processing pulses to (4-5). A further increase in the number of pulses does not lead to a significant increase in the modified layer thickness. As we can see from the table, within the statistical error, the thickness does not change with an increase in the number of pulses N>(4-5).
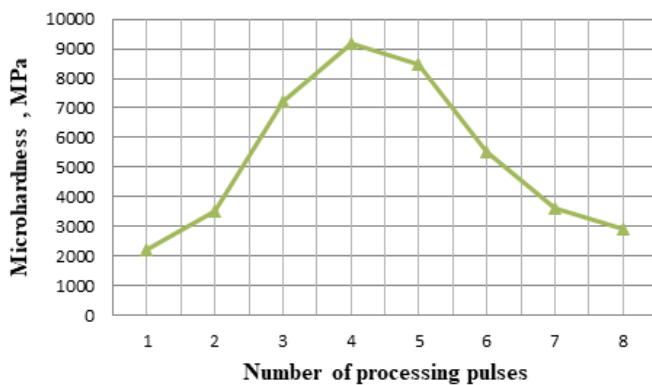

Figure 3. Dependence of the modified layer surface microhardness of 40X10C2M steel samples on the number of processing pulses

The dependence of the microhardness on the number of processing pulses was plotted for the optimal distance values from the source to the sample – of 30 mm and the discharge voltage – U = 4kV – Fig. 3.

The resulting curve correlates well with the data in the table: the thicker the homogeneous layer, the higher microhardness. The maximum microhardness value on the surface were also observed at 4 processing pulses.

For the processed samples, the microhardness values were determined at various points from the surface of the specimen cross-section into the depth of the modified layer. The microhardness curves are shown in Fig. 4 depending on the different number of processing pulses.

As we can see from Fig. 4, the position of the microhardness maximum depends on the plasma treatment modes. The microhardness maximum moves in depth when the number of processing pulses increases. For the number of pulses N = 2, the microhardness maximum (4700 MPa) is at a depth of 30 μm. With an increase in the number of pulses to N = 3, the microhardness maximum (7500 MPa) shifts to a depth of ≈40 μm; at N = 4, a strongly marked maximum (12900 MPa) is observed at a depth of ≈ 60 μm. With an increase in the number of pulses to N = 5, we observe a microhardness maximum (11200 MPa) at a distance from the surface of ≈ 80 μm.

The presented curves also show that the microhardness values for all samples grow at power density rise on the sample surface load. The microhardness of the modified layer at its maximum rises by about five times compared to the untreated surface.

NUMERICAL SIMULATIONS AND DISCUSSION

To compose a mathematical model of heat transfer, while taking into account the melting-solidification process of the near-surface layer, we used the classical equation of thermal conductivity with a modified density, specific heat, and coefficient of thermal conductivity [19]:

$$\rho c_p \frac{\partial T}{\partial t} = \frac{\partial}{\partial x}\left(k\frac{\partial T}{\partial x}\right) ,$$ (1)

where T is the temperature, t and x are the time and coordinate, respectively, k is the coefficient of thermal conductivity of the substance, ρ is the density of the substance, c_p is the specific heat at constant pressure.
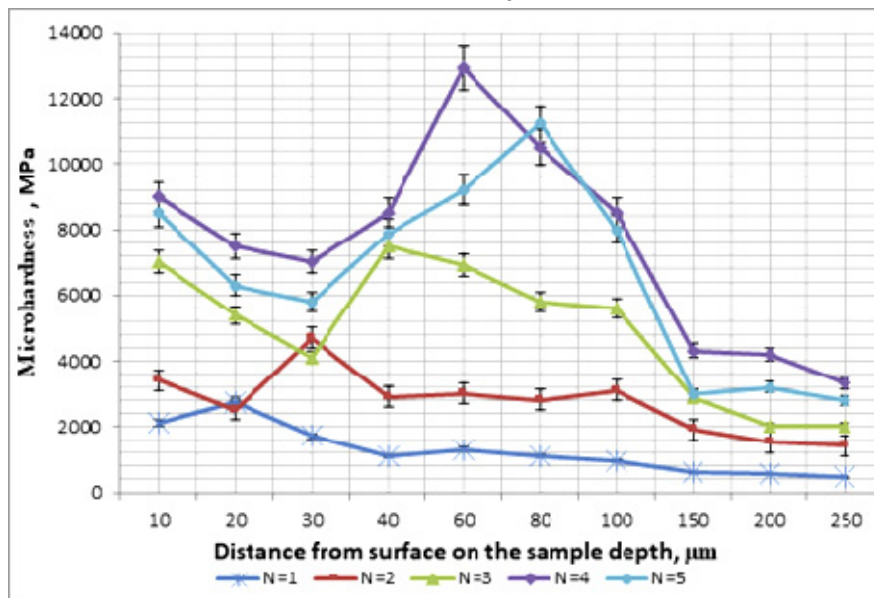

Figure 4. Microhardness dependence of the of 40X10C2M steel samples on the depth of the modified layer after a various number of processing pulses: curve 1 - the number of processing pulses N = 1; cr. 2 - N = 2; cr. 3 - N = 3; cr. 4 - N = 4; cr. 5 - N = 5. The discharge voltage is 4.0 kV, the distance from the sample to the plasma source is 30 mm.

The thermal conductivity coefficient was determined by the equation $k = (1-\theta)k_1 + \theta k_2$, where k_1 and k_2 are the thermal conductivity coefficients of the solid and liquid phases, respectively; α - a smoothing function that depends on the temperature T and simulates the two-phase state of the surface layer substance. The type of $\theta(T)$ is set on the assumption that the phase transition occurs in the temperature range from $T_{pc} - \Delta T/2$ to $T_{pc} + \Delta T/2$, where T_{pc} is the temperature of the metal-melt phase transition (melting point), ΔT is the width of the temperature range where the substance is in a two-phase state.

We define $\theta(T)$ in such a way that it is equal to one when the substance is a liquid and zero when it is a solid:

$$\theta(T) = \begin{cases} 0, & T \le T_p - \Delta T/2 \\ 1, & T \ge T_{pc} + \Delta T/2 \end{cases}.$$

In the case of an infinitely narrow interval ($\Delta T \to 0$), the function $\theta(T)$ is the Heaviside function equal to zero at $T < T_{pc}$ and is unity at $T > T_{pc}$.

For the specific heat at constant pressure, we applied the equation

$$c_p = \frac{(1-\theta(T))\rho_1 c_{p,1} + \theta(T)\rho_2 c_{p,2}}{(1-\theta(T))\rho_1 + \theta(T)\rho_2} + \lambda \frac{d\alpha(T)}{dT}$$

where λ is the specific heat of steel melting, $c_{p,1}$ and $c_{p,2}$ are the specific heat capacities of a solid and a melt, respectively; ρ_1, ρ_2 - are the density of the solid and liquid phases, respectively. Where $\alpha(T)$ – is the mass fraction

$$\alpha(T) = -\frac{1}{2}\frac{(1-\theta(T))\rho_1 - \theta(T)\rho_2}{(1-\theta(T))\rho_1 + \theta(T)\rho_2}$$

In this case, the condition $\int_{T_{pc}-\Delta T/2}^{T_{pc}+\Delta T/2} \frac{d\alpha(T)}{dT} dT = 1$ is met. In case of an infinitely narrow interval ($\Delta T \to 0$) $\frac{d\alpha}{dT}$ is – the Dirac function.

The substance density in (1) was given by the expression

$$\rho = (1-\alpha(T))\rho_1 + \alpha(T)\rho_2$$

Thus, in the presented model, there is a jump of the thermal conductivity coefficient, heat capacity, and substance density during the transition from a liquid to a solid phase. Taking this phenomenon into account leads to the fact that the heat equation (1) has a quasilinear character.

Within the chosen framework of the mathematical model, we carried out the numerical simulation of steel surface heating by rapid pulses, taking into account the melting and solidification of the substance in the Comsol Multiphysics package using finite element method. The mesh settings were fitted empirically to have a sufficient number of mesh nodes in the range with very rapidly changing values (first of all, the rate of temperature change dT/dt). The space step was taken equal to $2.5 \cdot 10^{-7}$ m, the maximum time -step was $2.5 \cdot 10^{-6}$ s. Table 2 shows the parameters for numerical calculations [20].

On the left boundary of the sample, we selected the following boundary condition

$$q(0) = f(t) \cdot q_0 - \sigma(T^4 - T_0^4) \tag{2}$$

where $q_0 = 10^9$ W/m^2 is the power density load on the sample irradiated surface, $f(t)$ is a function in the form of a smoothed rectangular pulse with a duration of 1.4 ms, T_0 is the temperature of the cold surface (room temperature), T is the temperature of the substance, σ is the Stefan-Boltzmann constant.

Table 2. Parameters of steel and steel melt for numerical simulation in the Comsol Multiphysics package.

Value Description	Notation	Value
Solid phase temperature (steel)	T_0	293 K
Liquid phase temperature (melt)	T_1	1480 ^{0}C
Transition temperature interval	ΔT	49 K
Specific heat of melting	λ	84 kJ/kg
Steel density	ρ_1	7620 kg/m^3
Melt density	ρ_2	7250 kg/m^3
Steel specific heat	$c_{p,1}$	532 J/kg·K
Melt specific heat	$c_{p,2}$	825 J/kg·K
Steel thermal conductivity coefficient	k_1	52 W/m·K
Melt thermal conductivity coefficient	k_2	22 W/m·K
Thickness of metal layer (specimen)	l	2 mm
Power density on the sample surface	q_0	10^9 W/m^2

At the initial moment of time, the temperature was the same and equal to T_0 throughout the sample. In the expression (2), the second term takes into account the energy loss at the sample boundary due to thermal radiation. Boundary conditions on the right (back) side of the sample $q(l) = -\sigma(T^4 - T_0^4)$. We didn't consider the reflection and evaporation process from the boundary.

Figs. 5-7 show the results of numerical simulations. Fig. 5 shows a non-standard behavior of the melt cooling rate - dT / dt: the rate at certain times reaches its maximum not on the surface (as is usually in the case of solid heating), but in the depth of ≈ 20 μm of the sample.

As it is known, at the highest metal cooling rate, the regions of increased hardness are formed in the processes of quenching and hardening. The positions of the cooling rate maxima are somewhat different from the experimental values of the microhardness maxima (30-80) μm. However, the qualitative variation of the dependencies in Fig. 5 correlates well with the experimental results.
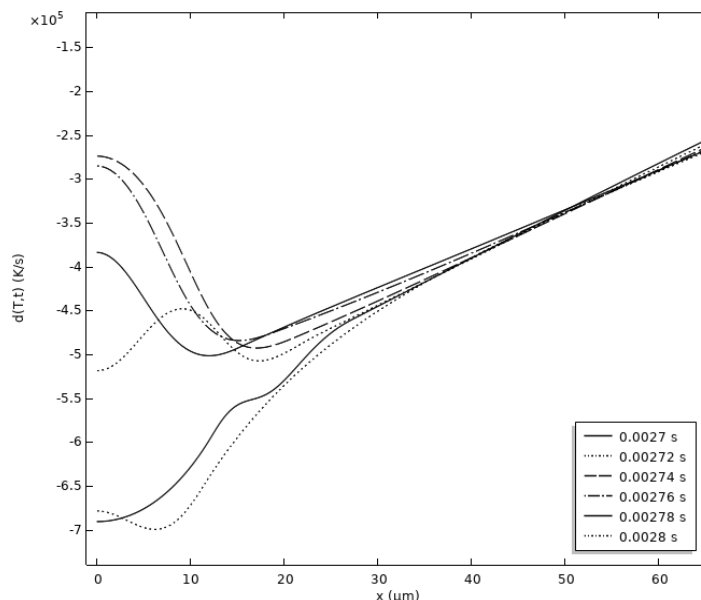

Figure 5. Dependencies of the temperature change rate (cooling rate) of the melt on the coordinate x deep into the sample for different points in time after the pulse power input: 0.00270 s, 0.00272 s, 0.00274 s, etc.
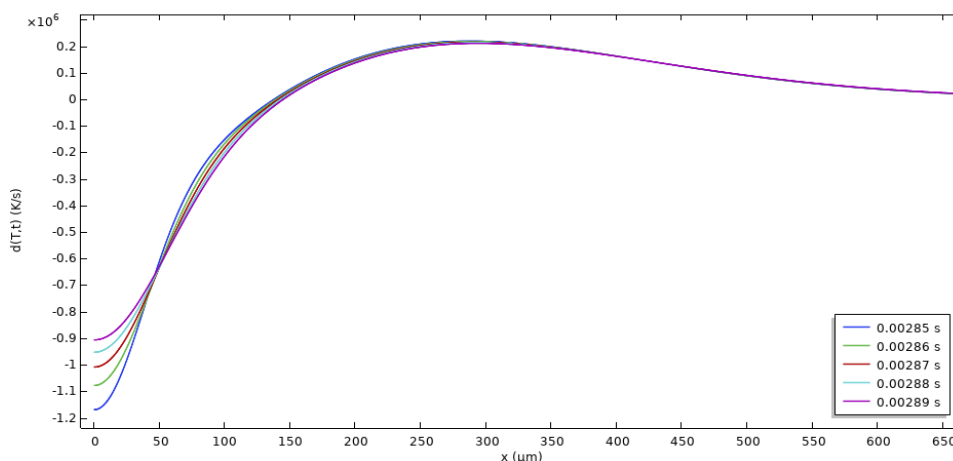

Figure 6. Dependencies of the temperature change rate (cooling rate) of the melt on the x coordinate into the depth of the sample for the moments of time 0.00285 s; 0.00286 s; 0.00287 s; 0.00288 s; 0.00289 s after impulse power input.

The regions of extreme cooling rates are preserved for the moment t = 0.00285 s when the complete solidification of the melt occurs. With the complete solidification of the sample, the zone of abnormally rapid cooling disappears, and the dependences of the temperature change rate dT / dt become monotonous – (Fig. 6). One can see that the cooling rate monotonically decreases from the surface into the sample's interior.

Fig. 7 shows the cooling rate dependence of the melt on the cooling time on the surface and several points in the depth of the sample.

One can see that at distances (15, 20, 30) μm from the surface deep into the sample for a certain period, the cooling rate has maxima which is much higher than the cooling rate on the surface (curve 0 μm in the figure), which corresponds to the creation of a maximum microhardness in the modified layer depth.

The results of numerical simulations also show that the cooling rate is a nonlinear function of time, which corresponds to our mathematical model, in which the thermal conductivity coefficient k is a nonlinear function. The

nonmonotonic dependence of the cooling rate on time also indicates the correctness of the two-phase model "melt-solid" chosen for modeling.

As one can see from the presented results (Fig. 5-7), the dependences obtained during modeling correlate well with the experimentally observed distribution of the modified layer microhardness.
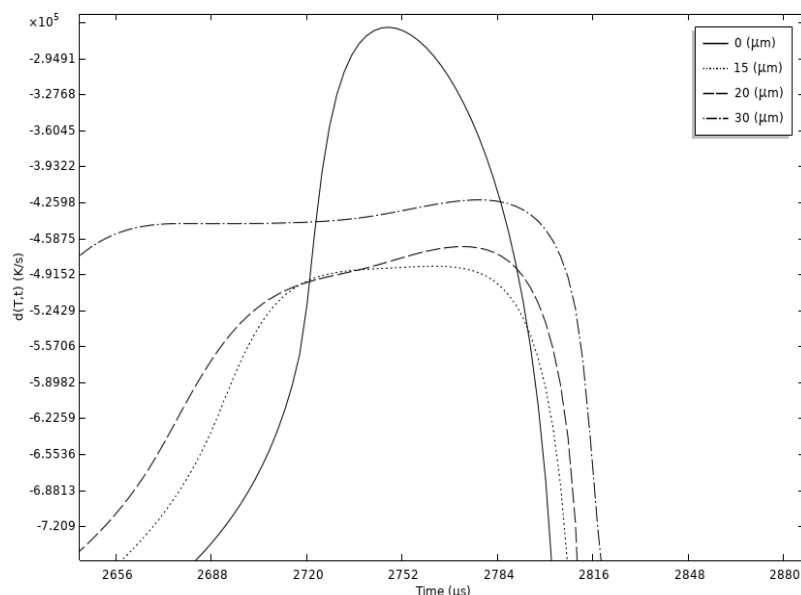

Figure 7. Dependencies of the temperature change rate (cooling rate) dT/dt of the melt on the cooling time on the sample surface (0 μm) and at various points deep into the sample (15 μm, 20 μm, 30 μm, etc.

The formation of microhardness maxima is in the depth of the modified layer and it shifts with increasing depth of the heat-affected zone "heating – cooling" can be explained as follows. It is known that the creation of a hardened layer on the surface occurs as a result of the ultrafast heating-cooling cycle due to two mechanisms: thermal radiation from the surface and the heat conduction mechanism deep into the sample. Due to the implementation of the first mechanism, a "traditional" microhardness maximum on the surface is formed. With a power density growth on the sample surface because of the formation of a molten zone, the second cooling mechanism is also activated - due to the release of heat during the transition of a material part from the liquid to the solid phase. Due to this mechanism, a second microhardness maximum is formed in the modified layer depth [21].

Microhardness growth is associated with structural changes during treatment process. The base of steel 40X10C2M in the initial hypoeutectoid state is ferrite with pearlite (α-Fe) with a BCC lattice. At the "heating and melting" stage, the surface layer temperature rises to $1480\,^{\circ}C$. This results in the transformation of pearlite into austenite (γ – Fe) and forming a phase with an FCC lattice [22]. The transition from the ferrite BCC-structure to the austenite FCC-structure is also facilitated by alloying the molten region with atoms and ions of the consumable iron cathode, nitrogen, oxygen, and other ionized air particles. Thus, at the heating stage, a highly alloyed two-phase solution of α-iron and γ-iron is formed, and the crystallites size of the treated steel ferrite component decreases. At the cooling stage, this solution is partially converted into martensite. As a result, a fine-grained austenitic-martensitic structure occurs, that is, a strengthened alloyed layer. Structural changes lead to substantial growth of layer hardness, microhardness increases by ≈5 times.

CONCLUSIONS

1. As a result of pulsed plasma treatment of the surface layer of 40X10C2M steel, a modified layer with improved operational properties is formed: the structure of this layer is homogeneous, without pores and cracks; the microhardness of the layer increases by ≈5 times.

2. We discovered a maximum of microhardness in the depth of the modified layer; the localization of the maximum depends on the modes of pulsed plasma treatment. By changing these parameters, it is possible to get the desired profile of the microhardness distribution along with the depth of the modified layer, which makes it possible to form specific operational characteristics of the treated layer.

3. We performed numerical simulations of the rapid pulsed heating of the surface layer using the two-phase model "melt - solid". We took into account the dynamics of the thermodynamic characteristics of steel. Within the chosen mathematical model framework, numerical simulation was carried out in the Comsol Multiphysics package by the finite element method.

4. We obtained a good agreement of simulation results with experimental data. The chosen computational model allowed us to obtain the character of the change in microhardness deep into the sample, which we observed experimentally.

ORCID IDs
Nikolay A. Savinkov, https://orcid.org/0000-0003-0549-7127; **Oleh M. Bulanchuk**, https://orcid.org/0000-0002-2801-2244;
Aleksander A. Bizyukov, https://orcid.org/0000-0003-0192-5219

REFERENCES

[1] Y. Zhao, B. Gao, G.F. To, S.W. Li, S.Z Zhao, and C. Dong, Applied Surface Science. **257**, 3913 (2011), https://doi.org/10.1016/j.apsusc.2010.11.118

[2] A.D. Pogrebnjak, and Y.N. Tyurin, Physics-Uspekhi. 48(5), 487 (2005), http://dx.doi.org/10.1070/PU2005v048n05ABEH002055

[3] A.D. Korotaev, Surface and Coatings Technology. **185** (1), 38-49 (2004), https://doi.org/10.1016/j.surfcoat.2003.11.021

[4] A.A. Skvortsov, S.G. Kalenkov, and M.V. Koryachko, Письма в ЖТФ [Letters in ZhTF], **40**(18), 24 (2014). (in Russian)

[5] E.V. Haranzhevskiy, D.A. Danilov, M.D. Krivilyov, and P.K. Galenko, Mater. Sci. Eng. A. **375**, 502 (2004), https://doi.org/10.1016/j.msea.2003.10.040

[6] A.G.M. Pukasiewicz, Jr.P.R. C. Alcover, A.R. Capra, and R.S.C. Paredes, Journal of Thermal Spray Technology, **23**(1-2), 51 (2014), https://doi.org/10.1007/s11666-013-0001-1

[7] Y.D. Shitsyn, D.S. Belinin, S.D. Neulybin, and P.S. Kuchev, Modern Applied Science. **9**(6), 64-75 (2015), https://doi.org/10.5539/mas.v9n6p64.

[8] E.S. Vaschuk, E.A. Budovsky, S.V. Raykov, and V.E. Gromov, Фундаментальные проблемы современного материаловедения [Fundamental problems of modern Materials Science]. **10**(1), 68-71 (2013). (in Russian)

[9] D. Karthik, S. Kalainathan, and S. Swaroop, Surface and Coatings Technology, **278**, 138 (2015), DOI:10.1016/j.surfcoat.2015.08.012

[10] E.A. Ochoa, D. Wisniveski, T. Minea, M. Ganciu, C. Tauziede, P. Chapon, and F. Alvarez, Surface and Coatings Technology, 203(10-11), 1457 (2009), https://doi.org/10.1016/j.surfcoat.2008.11.025

[11] V.D. Sarychev, S.V. Konovalov and B.B. Haimzon, Известия вузов. Чёрная металлургия [News of universities. Ferrous metallurgy]. 8, 52 (2011). (in Russian)

[12] S. Alavi, M. Passandideh-Fard, and J. Mostaghimi. Journal of Thermal Spray Technology. **21**, 248 (2012), https://doi.org/10.1007/s11666-012-9804-8.

[13] D.N. Trushnikov, D.S. Belinin, and Yu.D. Schitsyin, Современные проблемы науки и образования [Modern problems of science and education]. 2, 95 (2014). (in Russian), http://www.science-education.ru/ru/article/view?id=12706

[14] H. Qu, Ch. Wang, X. Guo, and A. Mandelis. Journal of Applied Physics. **104**(11), 113518 (2008), https://doi.org/10.1063/1.3035831.

[15] V.S. Verkhoribov, Yu.S. Korobov, S.V. Nevezhin, Yu.D. Shutsyn, and I.A. Gilev, Master's Journal. **1**, 81 (2015). (in Russian)

[16] W. Piekarska, and M. Kubiak. Applied Mathematical Modelling, **37**(4), 2051 (2013), https://doi.org/10.1016/j.apm.2012.04.052

[17] F.Kh. Mirzade, V.G. Niziev, V.Ya. Panchenko, M.D.Khomenko, R.V.Grishaevm, S.Pityana, and Corney van Rooyen, Physica B: Condensed Matter, **423**, 69 (2013), https://doi.org/10.1016/j.physb.2013.04.053

[18] Yu.E. Kolyada, A.A. Bizyukov, O.N. Bulanchuk, and V.I. Fedun, PAST, Series: Plasma Electronics and New Methods of Acceleration, **4**(98), 319 (2015), https://vant.kipt.kharkov.ua/ARTICLE/VANT_2015_4/article_2015_4_319.pdf

[19] C. Bonacina, G. Comini, A. Fasano, and M. Primicerio, International Journal of Heat and Mass Transfer. **16**, 1825 (1973), https://doi.org/10.1016/0017-9310(73)90202-0

[20] A. I. Volkov, and I. M. Zharvsky, *Большой химический справочник [Big chemical reference book]*, (Soviet School, Moscow, 2005), pp.608. (in Russian)

[21] N.A. Savinkov, and Yu.E. Kolyada, Вісник Приазовського державного технічного університету: Збірник наукових праць [Bulletin of the Priazovsky State Technical University: Collection of scientific works], **29**, 70 (2014). (in Russian).

[22] I.K. Razumov, Yu.N. Gornyostrev, and M.I. Katsnelson, Физика металлов и металловедение [Metal physics and metal studies], **118**(4), 380 (2017). (in Russian)

ВПЛИВ ІМПУЛЬСНОЇ ПЛАЗМОВОЇ ОБРОБКИ НА МІКРОТВЕРДІСТЬ СТАЛІ 40Х10С2М: ЕКСПЕРИМЕНТ І ЧИСЕЛЬНЕ МОДЕЛЮВАННЯ

М.О. Савінков[a,*], О.М. Буланчук[b], О.А. Бізюков[c]
[a]Азовський морський інститут НУ «ОМА», вул. Чорноморська 19 ., Маріуполь, 87517, Україна
[b]Донецький державний університет управління , вул. Карпінського 58, Маріуполь, 87513, Україна
[c]Харківський національний університет ім. В.Н. Каразіна, пл.Свободи 4, Харків, 61022, Україна

В роботі вивчаються експлуатаційні характеристики сталі 40Х10С2М, що застосовується для виготовлення елементів силових установок судна, після високоенергетичної імпульсної плазмової обробки**.** Для цього використовувався електротермічний плазмовий прискорювач, в камері якого ініціювався потужнострумовий імпульсний дуговий розряд високого тиску з параметрами: тривалість розряду - 1,4 мс, максимальний струм - 5 кА, напруга розряду до 5кВ. Досліджується мікротвердість і мікроструктура обробленого (модифікованого) шару. Визначено оптимальні параметри обробки сталі, які забезпечують найкращі характеристики модифікованого шару: мікротвердість збільшується в ≈ 5 разів. Виявлено максимуми мікротвердості в глибині модифікованого шару. Вивчаються можливість управління локалізацією максимумів, як способу формування потрібних експлуатаційних характеристик обробленого шару. Виконано математичне моделювання швидкого імпульсного нагріву поверхневого шару сталі в рамках двофазної моделі "розплав - тверде тіло" з урахуванням динаміки термодинамічних характеристик сталі. Для цього використовувалося класичне рівняння теплопровідності зі змінними параметрами сталі: густиною, теплоємністю і коефіцієнтом теплопровідності при переході речовини з рідкої в тверду фазу. В рамках обраної математичної моделі були зроблені чисельні розрахунки явища швидкого імпульсного нагріву поверхні сталі з урахуванням плавлення і затвердіння в пакеті Comsol Multiphysics з використанням методу скінчених елементів. Отримано добре узгодження результатів чисельного моделювання з отриманим в експерименті розподілом мікротвердості обробленого шару сталі вглиб зразка.

Ключові слова: плазмова обробка, модифікований шар, мікротвердість, мікроструктура, рівняння теплопровідності, плавлення і затвердіння, швидкість охолодження розплаву.